Improved Precision of MR Temperature Mapping of Mobile Organs Using Magnetic Field Modeling

G. Maclair[1,2], B. Denis de Senneville[1], M. Ries[1], B. Quesson[1], P. Desbarats[2], J. Benois-Pineau[2], and C. Moonen[1]
[1]Laboratory for Molecular and Functional Imaging, Bordeaux, Gironde, France, [2]LaBRI, Talence, Gironde, France

Purpose

Evaluation of magnetic field mapping as an alternative to multi-baseline reference maps for rapid processing of temperature images mobile organs.

Introduction

Real-time thermometry provides temperature monitoring inside the human body and is an interesting tool to control interventional therapies based on thermal ablation. The Proton Resonance Frequency (PRF) technique gives an estimate of temperature change at instant t (noted ΔT_t) by evaluating phase shifts between dynamically acquired images and reference data sets (1) [1]. The phase φ is directly proportional to the magnetic field $\vec{B}_0$. Since $\vec{B}_0$ is generally spatially non-uniform, any phase measurements on a tissue sample taken at different positions will show a relative phase difference potentially leading to severe errors in computed temperature maps [2]. Classic multi-baseline correction approaches use a complete collection of reference magnitude and phase images constructed before thermal therapy [3]. During the intervention, the phase image of the collection acquired with a similar organ position is selected (for that purpose, an inter-correlation coefficient can be computed for anatomical images), and then used as a reference for temperature computation in equation (1). However, the correction is constrained to positions present in the collection and complex motion patterns require a densely populated collection. Thus computational overhead may be unsuitable for real-time MR-thermometry.
The alternative correction method described in this paper consists of two steps: a linear magnetic field perturbation model is computed in a preparative step; subsequently, during the intervention, this model is used to reconstruct the magnetic field perturbation corresponding to the actual organ position in real-time which in turns allows computation of motion corrected thermal maps.

Material and Methods

Preparative learning step: This step is performed before the intervention (no hyperthermia, same MR acquisition protocol). A training set N flow fields relating complex organ deformation is estimated on anatomical images using an image registration algorithm [4]. From this set, a small parameterized motion flow model D_i, $0 \le i < m$ (typically m=5) is constructed using a Principal Components Analysis. The spatial transformation T_t between the actual anatomical image I_t and the reference image I_0 is thus a linear combination of D_i (2). The small set of parameters C_i^t, which gives an optimal representation of the actual complex organ deformation, can then be computed by minimizing (3) using a Marquardt-Levenberg least square solver [4].

Modeling motion induced phase changes: The overall magnetic field variation is approximated by a sum of linear phase changes of each principal motion component on a pixel-by-pixel basis (4). P_i, $0 \le i < m$, which denotes the parameterized magnetic field model, is computed at the end of the preparative step, using a Singular Value Decomposition (SVD) applied on the overdetermined set of N equations and $m+1$ unknowns reported in (4).

Hyperthermia procedure: The parameterized magnetic field model P_i and the set of parameters C_i^t representing the actual organ displacement allow the reconstruction of phase distribution φ_{reco} corresponding to the actual organ position with equation (5). φ_{reco} is then used as reference for temperature computation with equation (1).

$$\Delta T_t = (\varphi_{ref} - \varphi_n).Const\_PRF \quad (1)$$

$$T_t(x,y) = \sum_0^{m-1} C_i^t D_i(x,y) \quad (2)$$

$$LS = (I_0 - T_t(I_t))^2 \quad (3)$$

$$\varphi_t(x,y) = \sum_{i=0}^{m-1} C_i^t P_i(x,y) + P_m(x,y) \quad \forall t, 0 \le t \le N-1 \quad (4)$$

$$\varphi_{reco}(x,y) = \sum_{i=0}^{m-1} C_i^t P_i(x,y) + P_m(x,y) \quad (5)$$

Results and Discussion

All experiments were performed on a Philips Achieva 1.5 Tesla MR scanner. On the first experiment, temperature stability and model validity was analysed on the abdomen of a healty volunteer under free breathing (resolution: 128×128, TR=100ms, TE=28ms, learning step: 50 images).

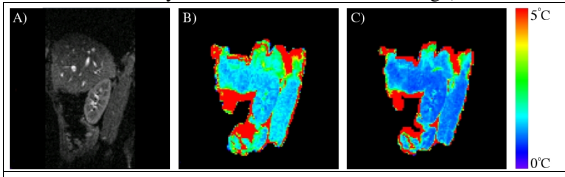

Figure 1. *Temperature standard deviation maps obtained on the abdomen of a free breathing volunteer. A) anatomical image, B) classic multi-baseline approach [3], C) proposed correction.*

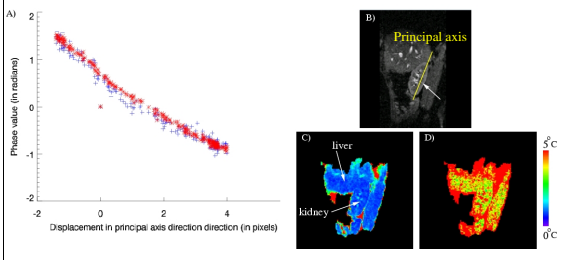

Figure 2. *Quality criteria for the magnetic field modeling: A) phase variation along the principal axis reported by the yellow line on B) in a pixel located in the kidney (white arrow). In blue the measured phase values, in red the reconstructed phase values; C) temperature standard deviation error over the entire experiment at a constant body temp. of 37°C; D) SVD Pi(x,y) estimation error as a validity map of the field model expressed as peak-to-peak temperature error.*

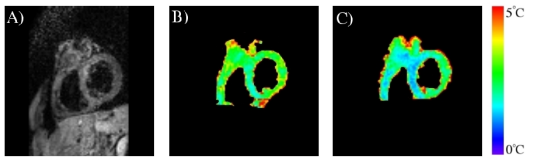

Figure 3. *Temperature standard deviation maps obtained on heart a healthy volunteer under free breathing: A) anatomical image, B) classic multi-baseline approach [3], C) proposed correction.*

It can be observed on **Figure 1** that the proposed approach gives an accurate temperature monitoring both the kidney and the liver. Note that, with the proposed approach, temperature uncertainty will be optimally reduced with a factor $\sqrt{2}$ compared to mutli-baseline approach (as P_i results from an overdertermined system, and, thus, optimally, $\sigma(\varphi_{reco})$=0). This was observed in practice as 1.5°C and 1.1°C of temperature uncertainty were respectively measured with the multi-baseline and the proposed approach.
The data shown in **Figure 2** confirms the linearity assumption of the phase changes with respect to the motion pattern prevalent in this study. Furthermore, the measures C) and D) provide quality criteria of the magnetic field modeling and can be used to quantify the accuracy of our magnetic field model.
Figure 3 shows preliminary results of the proposed method obtained with a cardiac triggering sequence on a healthy volunteer under free breathing. An improvement of the temperature accuracy can also be observed for these results offering great perspectives for on-line cardiac temperature imaging.

Computational time required on a a dual processor dual core AMD Opteron 2.4 GHz with 8 Gb of RAM for classical multi-baseline and proposed approach were respectively 150ms and 75ms.

Conclusion

The proposed approach presents several advantages compared to the existing multi-baseline approach: improvement of accuracy on temperature maps, an improved robustness with respect to local and global intensity changes, and a non-negligible computational time acceleration that makes the proposed work compatible with the real-time thermotherapy constraint.

References

[1] De Poorter J. et al. MRM 1995;33(1):74-81.
[2] Young I. R. et al., MRM 1996;36(3):366-74.
[3]Denis de Senneville B. et al., MRM 2007;57:319-30.
[4] Maclair G., et al., IEEE, ICIP 2007, vol.III, 141-144.